Journal of Materials Science: Materials in Electronics (2018) 29:3006–3013
https://doi.org/10.1007/s10854-017-8231-5

Green emission from a Eu^{2+}-activated $SrAl_2O_4$ phosphor: a photoluminescence and electron spin resonance study

Vijay Singh[1] · N. Singh[1] · M. S. Pathak[1] · Hakyung Jeong[2] · S. Watanabe[3] · T. K. Gundu Rao[3] · V. Dubey[4] · V. K. Rai[5]

Received: 19 September 2017 / Accepted: 7 November 2017 / Published online: 18 November 2017

Abstract
$SrAl_2O_4Eu^{2+}$ green-light emitting powder phosphor was prepared within a few minutes at furnace temperature as low as 550 °C by using combustion method. The prepared powder was characterized by X-ray diffraction, scanning electron microscopy and Fourier-transform infrared spectrometry. Several ESR lines are exhibited by the phosphor, and some are seen in the low field region apart from lines in the g ~ 2.0 region. Crystal fields that were relatively strong arose from distortions close to the Eu^{2+} ion lead to lines in the low field region. The photoluminescence of Eu^{2+}-activated $SrAl_2O_4$ shows a green-emission dominant peak around 514 nm, which can be attributed to the $4f^65d^1 \rightarrow 4f^7$ transition of Eu^{2+} ions from the synthesized phosphor particles at an excitation wavelength of 345 nm.

1 Introduction

Rare-earth and transition-metal-ion-doped alkaline earth aluminates have been widely investigated due to their excellent physical, optical and eco-friendly properties [1–3]. The alkaline earth aluminates phosphors doped with rare earth ions are functional inorganic materials that exhibit strong luminescence properties. These materials have attracted much attention in terms of the range of their applications, such as display devices, signage, medical applications, emergency rescue guidance systems, and storage devices [4–6]. In addition, these systems have been known to be excellent long-persistence phosphors due to their high efficient luminescence centers and potential to emit light a long time after the excitation has ended [7, 8]. Strontium aluminate ($SrAl_2O_4$) phosphors, in particular, have been investigated widely due to their persistent phosphorescence with high quantum efficiencies and good chemical stabilities [9]. Strontium aluminates doped with Eu^{2+} ions are finding use in a variety of applications such as luminous paints, emergency lighting, safe traffic, wall painting, films, artificial fibers, rubbers, textiles ceramics, lamp industry, color display, radiation dosimetry, X-ray imaging [10]. $SrAl_2O_4$ co-doped with Eu^{2+} and Dy^{3+} have been extensively investigated due to their excellent properties. The materials can be used in construction to detect damage to bridges, low-level escape systems during general power failures, textile printing, clock watches, electronic dial plates, and luminous paints [10–13].

$SrAl_2O_4$ belongs to the large family of stuffed tridymite structures which consists of corner-sharing AlO_4 tetrahedrons, with each oxygen shared with two aluminum ions and a Sr^{2+} cation that occupy interstitial sites within the tetrahedral frame work. It is known that at room temperature, $SrAl_2O_4$ is monoclinic, with a $P2_1/n$ space group and, at high temperatures, it is hexagonal, with a $P6_322$ space group. Structural phase transitions occur between these two types of structures during cooling. Strontium aluminate has conventionally been synthesized by a solid-state method at high temperature, but nowadays $SrAl_2O_4$ is prepared by low-temperature synthetic techniques such as chemical precipitation, combustion synthesis, and a sol–gel process. A spray pyrolysis method and a reversed micelles method have been reported to synthesize strontium aluminate phosphors

✉ Vijay Singh
vijayjiin2006@yahoo.com

[1] Department of Chemical Engineering, Konkuk University, Seoul 05029, South Korea

[2] Department of Mechanical Design and Production Engineering, Konkuk University, Seoul 05029, South Korea

[3] Institute of Physics, University of Sao Paulo, São Paulo, SP 05508-090, Brazil

[4] Department of Physics, Bhilai Institute of Technology, Kendri, Raipur 493661, India

[5] Laser and Spectroscopy Laboratory, Department of Applied Physics, Indian Institute of Technology (Indian School of Mines), Dhanbad, Jharkhand 8260041, India

[14–19]. Strontium aluminate has been known to be an efficient host material with broadband emissions.

The Eu^{2+} shows a large absorption of ultraviolet (UV) light and a broad emission, ranging from UV to red light due to a $4f^6 5d^1 - 4f^7(^8S_{7/2})$ transition, depending on different crystal-lattice environments. The green-emitting Eu^{2+}-doped phosphor has been widely investigated. Zhong et al. [20] reported the synthesis and spectroscopic investigation of $Ba_3La_6(SiO_4)_6:Eu^{2+}$ green phosphors for white light-emitting diodes. Xia et al. [21] reported $Ca_6La_4(SiO_4)_2(PO_4)_4O_2:Eu^{2+}$, a novel apatite green-emitting phosphor. Lü et al. [22] investigated near-UV and a blue-based LED fabricated with $Ca_8Zn(SiO_4)_4Cl_2:Eu^{2+}$ as a green-emitting phosphor. Komukai et al. [23] studied a high-luminescence $BaZrSi_3O_9:Eu^{2+}$ blue-green-emitting phosphor. Li et al. [24] reported a $Ba_3Si_6O_{12}N_2:Eu^{2+}$ green-emitting phosphor for white LEDs. The aluminate of interest in the present study is Eu^{2+} activated $SrAl_2O_4$ phosphor.

Electron spin resonance (ESR) spectroscopy, in particular, is a very important method that allows the establishment of the symmetry of the paramagnetic center and the charge state. In this regard, the aim of this investigation was, therefore, to study the ESR of the Eu^{2+} activator in $SrAl_2O_4$ powder phosphor. The combustion process is fast, simple and safe and requires a low temperature for preparation of phosphors as materials. Taking this point into account, in the present paper, we have successfully prepared $SrAl_2O_4$:Eu phosphor at a relatively low temperature via a solution-combustion process. The prepared phosphor was well characterized by X-ray diffraction (XRD), scanning electron microscopy (SEM), Fourier transforms infrared (FT-IR), electron spin resonance (ESR) and photoluminescence (PL) techniques.

2 Experimental

Eu^{2+}-doped $SrAl_2O_4$ crystals aluminates were prepared with the chemical formula $SrEu_{0.01}Al_2O_4$ by a solution-combustion process (Source materials were: 0.5641 g $Sr(NO_3)_2$, 2.0 g $Al(NO_3)_3{\cdot}9H_2O$, 3.900 g $CO(NH_2)_2$, 0.0114 g $Eu(NO_3)_3{\cdot}5H_2O$). 0.0309 g of H_3BO_3 was used as a flux. To perform the combustion reaction, the starting materials were placed in a 100 ml glass beaker and mixed with a minimum amount of deionized water. The reaction was carried out in solution at 80 °C for 20 min to obtain a homogenous solution. Then the solution was introduced into a muffle furnace preheated to 550 °C. Initially, the solution was boiled and underwent a dehydration process. This was followed by decomposition with the evolution of large amounts of gas. The mixture was then frothed and swollen, thus forming a foam which burst into a flame and glowed to incandescence. During incandescence, the foam underwent further swelling to the capacity of the container. The entire combustion process was completed in less than 5 min. The beaker was taken out, and the foamy product was crushed into a fine powder. This powder was white in color and its properties were evaluated.

X-ray diffraction data were recorded at room temperature on a X'Pert Pro Diffractometer (Panalytical) using CuKα radiation in the 2θ range of 10° to 80°. Powder morphology was studied using scanning electron microscopy (SEM, Hitachi S-3200N, Japan). Fourier transform infrared (FT-IR) was performed with Thermo-Nicolet equipment in the range of 400–4000 cm^{-1}. The photoluminescence emission and excitation spectra of the samples were recorded by using a spectrofluorophotometer (RF-5301PC SHIMADZU) equipped with a Xenon lamp. A powdered sample of 100 mg was placed in a quartz tube for the ESR measurements. The ESR spectra of the sample were recorded on a JEOL FE1X ESR Spectrometer, operating in the X-band frequencies, with a field modulation of 100 kHz.

3 Results and discussion

3.1 X-ray diffraction studies

Figure 1 shows the X-ray diffraction peak of Eu^{2+}-doped $SrAl_2O_4$. All peaks are in good agreement with the joint commission standard pattern for $SrAl_2O_4$ (JCPDS File No. 74-0794) and (JCPDS File No. 31-1336) for monoclinic and hexagonal phases, respectively. It is well known that $SrAl_2O_4$ had two phases, depending on the temperature: below 650 °C the monoclinic form is stable, and above this temperature, $SrAl_2O_4$ crystallizes with hexagonal symmetry [25]. From the XRD it was confirmed that the

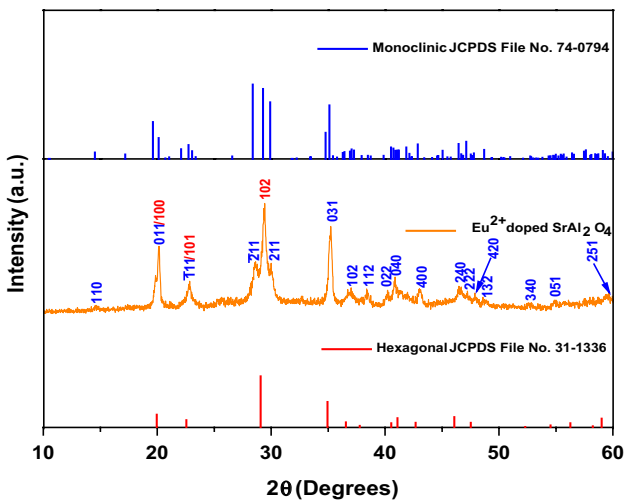

Fig. 1 XRD pattern of $SrAl_2O_4:Eu^{2+}$ phosphor

small amount of Eu^{2+} had no effect on the $SrAl_2O_4$ phase composition. We can simply assume that the ionic radii of Eu^{2+} (1.3 Å) are roughly equivalent to that of Sr^{2+} (1.31 Å) so that Eu^{2+} ions can easily substitute for Sr^{2+} sites and have no effect on the $SrAl_2O_4$ phase composition [26]. We have used a combustion method to obtain a crystalline phase of $SrAl_2O_4$ which requires much lower furnace temperatures compared to the solid-state method. The crystallite size was calculated by applying the well-known Scherer's equation: $D = 0.9\ \lambda/\beta\ \cos\theta$, where λ is the wavelength of incident X-ray, β is the FWHM of the main peak and θ is the corresponding Bragg's diffraction angle. The crystallite size calculated from this method is found to be 29.39 nm.

3.2 FT-IR

Figure 2 shows the FT-IR spectrum of the $SrAl_2O_4$:Eu powder. Absorption band arising from O–H stretching vibration of water occur at ~ 3650 to 3400 cm^{-1}. The sample shows the peak at ~ 1500 cm^{-1}. The peak of our sample at ~ 1500 cm^{-1} is in good agreement with the measurements of Misevicius et al. [27]. Misevicius et al. reported that the exact origin of this peak, however, is not very clear. Importantly, in the 1000–400 cm^{-1} fingerprint region, several sharp bands are observed due to typical metal–oxygen absorptions (Sr–O and Al–O stretching frequencies) [2, 27].

3.3 SEM

The SEM micrographs of the Eu^{2+}-activated $SrAl_2O_4$ phosphor is shown in Fig. 3a–f. Morphology of the prepared powder shows that the particles are overlapped and aggregated. The size of is also irregular with different shapes. The enlarged view of Fig. 3b (zone b) is shown in Fig. 3c. Particles with pores and voids are clearly visible on the enlarged image. A large amount of gas escaped as a result of the combustion reaction. Figure 3d shows that the particles also possess crystal and plate-like morphologies. The plates are irregular in shape and size. Both small and large plates are present. The enlarged view of Fig. 3e (zone e) is shown in Fig. 3f. From this image, it can clearly be observed that the plates are composed of nano-sized needles. Features inherent to the combustion product include pores, voids, plates, and needles.

3.4 Electron paramagnetic resonance studies

The ESR spectrum recorded at room temperature of the europium-doped $SrAl_2O_4$ phosphor is shown in Fig. 4. Several lines are seen mainly in the low field region of the spectrum, and the dominant lines are observed at $g \approx 18.5$, 6.3, 4.2, 2.99, 2.93, 2.025 and 1.99. Other lines have g-values

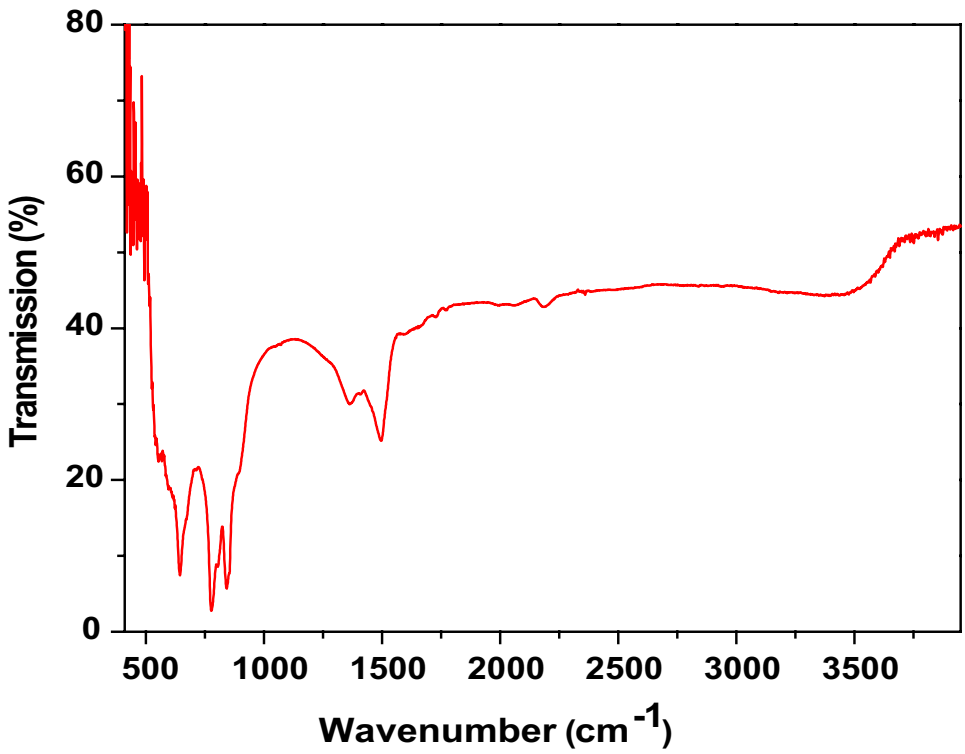

Fig. 2 FT-IR spectrum of $SrAl_2O_4$:Eu^{2+} phosphor

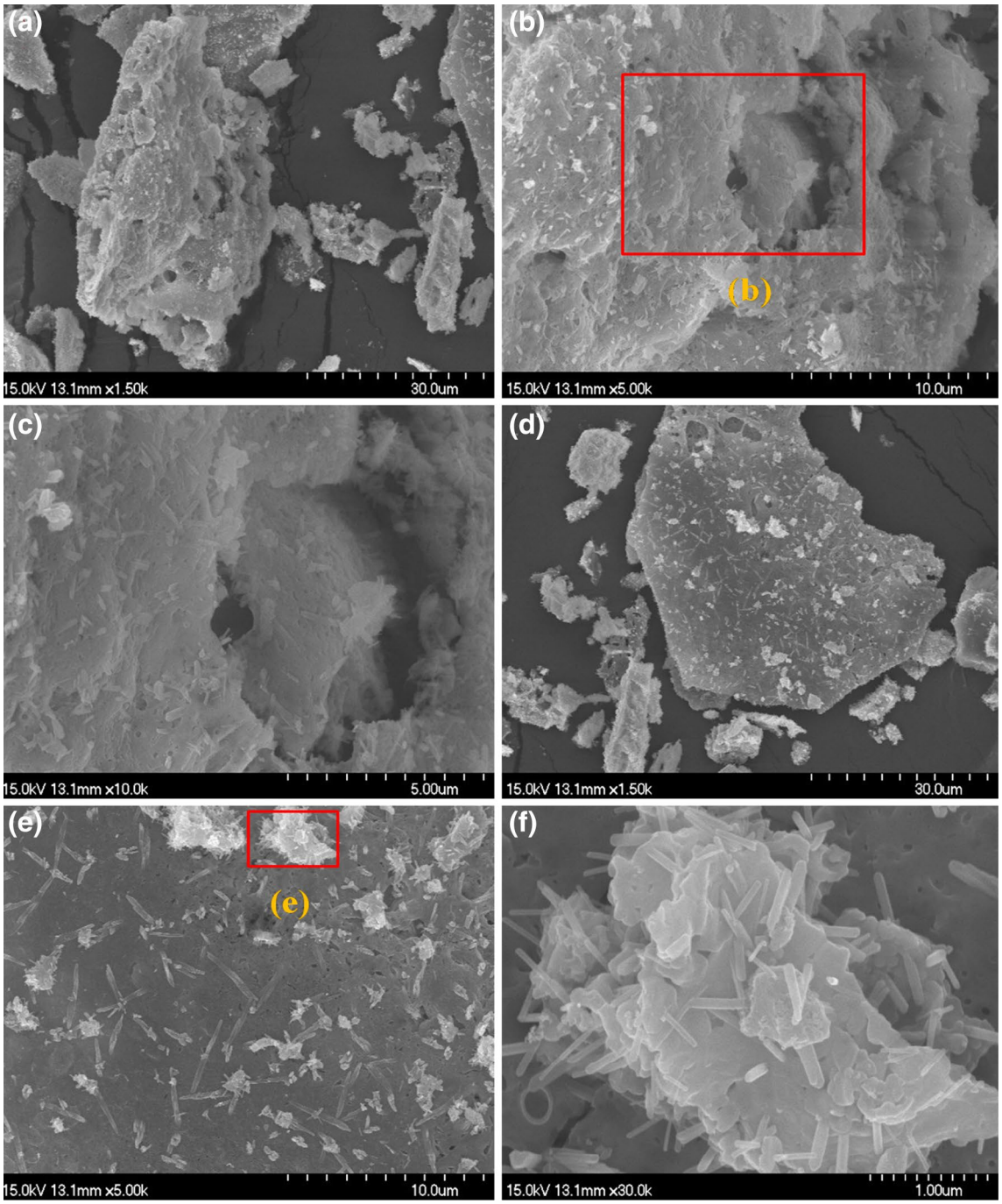

Fig. 3 SEM images of $SrAl_2O_4:Eu^{2+}$ phosphor

equal to 9.9, 4.4. Compared to other rare-earth ions, the Eu^{2+} ion is characterized by a relatively long relaxation time, and this makes it possible to observe its ESR spectrum at ambient temperatures. A normal ESR spectrum of the ion consists of seven equally spaced fine structure lines in case crystal field interaction is small compared to the microwave energy at 10 GHz. Nearest neighbors of the europium ion and the local symmetry strongly influences the separation between these fine structure lines. Due to the hyperfine interaction of the unpaired electron with Eu^{2+} (I = 5/2) nucleus, each of the seven fine structure lines splits into six lines. As there are two stable isotopes of europium (^{151}Eu and ^{153}Eu), there will be two sets of six hyperfine lines in the spectrum. S-state rare-earth ions Eu and Gd in polycrystalline powder systems exhibit typical ESR spectra which are quite different from those of glassy or disordered systems like zeolites [28, 29].

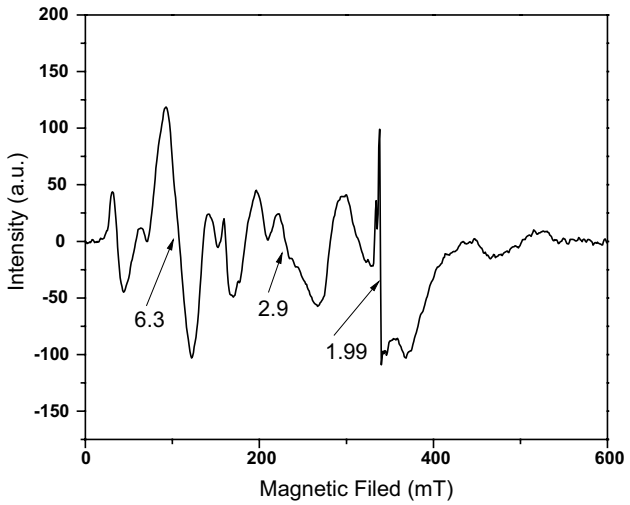

Fig. 4 ESR spectrum of $SrAl_2O_4$:Eu^{2+} phosphor

However, in some cases, even for materials which are crystalline, there can be occurrence of the disorder in certain lattice sites which can result in the distribution of crystal field experienced by the europium ion and the situation could be like that of a glassy material (polycrystalline $Pb_{1-(3/2)x}La_xZr_{1-y}TiO_3$) [29]. The observed spectrum in the present case appears to be similar to spectra of disordered or glassy systems.

Eu^{2+} and Gd^{3+} ions are different in the category of rare-earth ions as they have half-filled 4f shells. The electronic configuration of these ions is $[Xe]4f^7$. The ions have $L=0$ as they are pure S-states. Consequently, they have spherically symmetric charge clouds. This makes the ion unaffected by the crystal field caused by the nearest neighbor ions. Therefore, crystal field interactions will be extremely small. However, higher order perturbations are present and lead to perceptible crystal field effects. These perturbations arise from spin–orbit coupling and result in splitting of the states. Examples of higher states with $L\neq 0$ are $^6D_{7/2}$ and $^6P_{7/2,}$ and these states are mixed with the ground state which is a pure S-state. This mixing mediated by spin–orbit coupling enables the ion to interact with the crystal field. It should be emphasized that there is no direct coupling between the ion and the crystal field. The interaction gives rise to a splitting of the ground state. These splitting states are manifested as crystal field effects in the observed ESR spectrum. The symmetry of the lattice site occupied by a Eu^{2+} ion is determined by nearest neighbor ions. As the location and orientation of these neighboring ions change, there will be a corresponding change in the local symmetry at Eu^{2+} ion site. Local symmetry variations will cause a change in the magnitude of the crystal field at the ion, and there will be a corresponding change in the observed ESR spectrum.

Eu^{2+} and Gd^{3+} ions exhibit a unique ESR spectrum in glass systems, disordered lattices and some special cases of polycrystalline powder samples. A spectrum which has some similarities to this unique spectrum is also displayed by the Eu^{2+} ion in the present $SrAl_2O_4$:Eu^{2+} phosphor. Brodbeck and Iton [30] describe this kind of spectrum as a U-spectrum. Some of the explanations given earlier consider the Eu^{2+} ion to experience strong crystal fields when the ion is in low coordinated sites resulting in a weak shoulder line at $g\sim 4.2$. For the case of an ion with a high coordination number, lines are expected at $g=5.6$, 2.6 and 1.96. Despite these explanations, the reasons are believed to be not all that satisfactory. On the other hand, Brodbeck and Iton [30] give a more meaningful explanation for the U-spectrum. They consider the magnitude of crystal field interaction (H_{CF}) and Zeeman splitting $h\nu$ (where ν is the microwave frequency). This consideration allows Brodbeck and Iton to classify the observed ESR spectrum into different regions, viz., weak, intermediate and strong crystal field regions. Weak crystal field region corresponds to the case where $H_{CF}/h\nu \leq$ ¼. ESR lines are mostly confined to the free-electron region ($g\sim 2.0$). Intermediate region is divided into lower intermediate crystal field region and higher intermediate region. In the lower region $1/4 \leq H_{CF}/h\nu \leq 1$. Here ESR lines are expected over a wide range of g-values extending from 2.0 to ∞. Strong crystal field corresponds to the case where $H_{CF}/h\nu \geq 4$ and ESR lines are determined by transitions within the Kramer's levels.

$SrAl_2O_4$ crystallizes in the monoclinic structure with space group $P2_1/n$ [31]. $SrAl_2O_4$ is formed by a framework of corner-sharing AlO_4 tetrahedral. This framework results in the formation of cavities. The structure is derived from stuffed tridymite structure where all the Si^{4+} ions are replaced by Al^{3+} ions. The presence of Al^{3+} creates charge imbalance which is compensated by placing Sr^{2+} ions in the cavities which restore charge balance. Sr^{2+} ions are coordinated by nine oxygens and occupy two different sites.

The presence of divalent Sr^{2+} ion and trivalent Al^{3+} ion in the lattice brings out mixed occupancy where Al ions are partially replaced by divalent ions. This kind of cation exchange results from antisite cation exchange. This is also termed as cation exchange disorder and is a point defect in crystals. These defects are predicted to be present in the lattice by theoretical calculations [32]. X-ray diffraction [33] and X-ray absorption fine structure [34] investigations support the presence of such defects. On the other hand, they are also directly observed by high-angle annular dark-field (HAADF) and annual bright-field scanning transmission electron microscopy [35]. Two Sr sites exist in the $SrAl_2O_4$ system, and the dopant Eu ion is expected to substitute both these sites. This has been confirmed experimentally by low-temperature luminescence studies of Eu^{2+}-doped $SrAl_2O_4$ [36].

The ionic radius of Sr^{2+} ion in nine-fold coordination is 1.31 Å. The ionic radius of Eu^{2+} ion in the same coordination is 1.3 Å and is almost the same as Sr^{2+} ion radius [37]. On the other hand, the ionic radius of Al^{3+} ion (0.39 Å) is small and therefore, Eu^{2+} ion substitutes Sr^{2+} sites in the $SrAl_2O_4$ system. There is a possibility of formation of oxygen vacancies in the lattice due to cation disorder mentioned earlier and also due to non-stoichiometry. Theoretical calculations predict an ease of formation of oxygen vacancies when cation disorder is present in the lattice compared to a perfect cation-ordered system [38]. Oxygen vacancies located near Eu^{2+} ions may bring changes in the symmetry of the substitutional sites and lead to distortions. Distortions, in turn, alter the crystal field and make the Eu^{2+} ion experience stronger crystal fields. ESR lines will appear in the lower field region of the spectrum which is expected in the case of intermediate crystal fields discussed earlier.

It is observed that ESR lines are also seen near g = 2.0 region in Eu^{2+} doped $SrAl_2O_4$. Oxygen vacancies could be in positions which are far from certain Eu^{2+} ions. These ions would then be not perturbed by vacancies, and the local symmetry would be preserved leading to lines in the free-electron region.

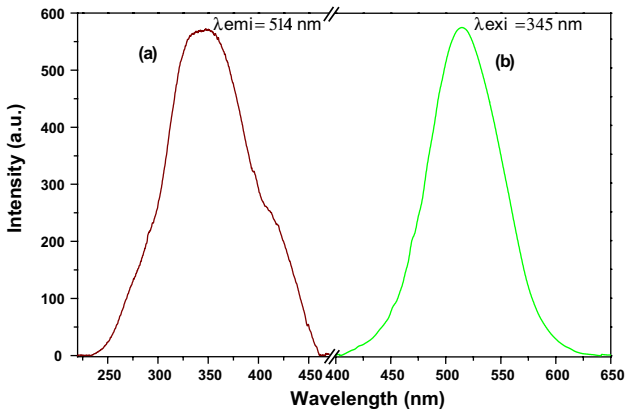

Fig. 5 Typical photoluminescence spectra of $SrAl_2O_4$:Eu^{2+} phosphor

3.5 Photoluminescence studies

The photoluminescence excitation and emission spectra of europium doped $SrAl_2O_4$ phosphor are shown in Fig. 5. The excitation spectrum of this phosphor is recorded by keeping the emission wavelength fixed at 514 nm. The observed absorption peak at 345 nm is assigned to the characteristic $4f^7 \rightarrow 4f^6 5d^1$ transition of the Eu^{2+} ions. Keeping the excitation wavelength fixed at 345 nm, the emission spectrum of this phosphor includes a broad band peak at 514 nm with a full width at half maximum about 77 nm is observed, which is typical of the $4f^6 5d^1 \rightarrow 4f^7$ emission of the Eu^{2+} ions. In $SrAl_2O_4$, Eu^{2+} could easily substitute for Sr^{2+} ions with comparable ionic radius and same charge. A broad band in the region 400–625 nm was observed in the present study, peaking at an emission wavelength of 514 nm. This result indicates that the prepared powder emit green light. The photo image shown in Fig. 6 confirms this point. It is worth to mention that the green emitting phosphor can be prepared by the combustion synthesis, which is simpler, safer, more energy saving way and within a shorter time compared to the solid-state reaction method. It is well known that the emission of Eu^{2+} is attributed to the transition from $4f^6 5d$ to the ground state $4f^7$. The 4f electrons are not sensitive to the crystal lattice environment, while the 5d electrons may easily couple with crystal lattice. Thus, the 4f5d state can be split by the influence of crystal field and coupled strongly with crystal lattice phonon, which leads to a broadband absorption and emission. The emission band of our sample at 514 nm is in good agreement with the measurements of Ravichandran et al. [39] who observed the band at 512 nm. However, the emission from $SrAl_2O_4$ was observed as a symmetrical band at 514 nm, a slightly shorter wavelength than the 518 nm observed by Song et al. [40] and 521 nm, observed by Palilla et al. [41]. In the present study, green emission band position at 514 nm may be due to the mix phase as we know emission of Eu^{2+} is due to interconfigurational d-f transitions, the energy of the emission strongly depends on the host material. In addition, the existence of an

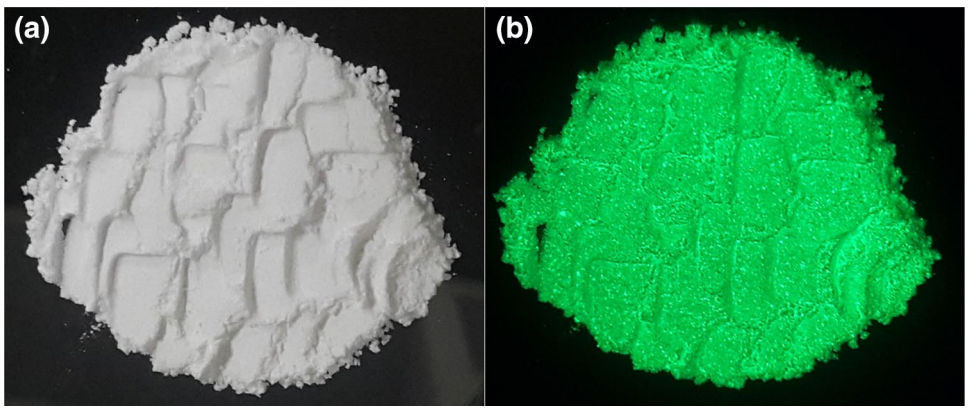

Fig. 6 Typical photographs of $SrAl_2O_4$:Eu^{2+} phosphor sample under a room light (appearance: **a** white powder) and **b** UV 365 nm (appearance: a green emission of Eu^{2+})

impure phase in $SrAl_2O_4$:Eu greatly affected its luminescent property. A detailed analysis was done and presented as the ESR study of the prepared sample. The incorporation and stabilization of Eu ions in the sample were confirmed by the ESR and luminescence investigations. Both the analysis of the sample confirms the presence of Eu^{2+} in the $SrAl_2O_4$ matrix.

Figure 7 displays the color coordinate of the emitted color from the $SrAl_2O_4$:Eu^{2+} after excitation via 345 nm wavelength. Herein the broad emission peak of the vacancy state of Eu^{2+} ion in the $SrAl_2O_4$ host will emit green light emission. Therefore, Commission Internationale de l'eclairage (CIE) coordinate of the phosphor is calculated. The coordinate is shown as (0.23, 0.50) which is close to green light emission. It shows the applicability of the emitted color for green emitting appliances.

4 Conclusions

$SrAl_2O_4$:Eu^{2+} phosphor was prepared by a combustion synthesis reaction at a furnace temperature 550 °C in an open atmosphere. The prepared sample was analyzed by XRD, SEM, FT-IR, PL and ESR measurements. ESR lines are observed near the free-electron region (g = 2.0) as well as in the low field region. Charge-compensator oxygen vacancies situated close to Eu^{2+} ion as well as in far locations may give rise to the observed spectrum. The luminescence spectra recorded at an excitation wavelength 345 nm exhibited emission bands at around 514 nm correspond to the transitions $4f^65d^1 \rightarrow 4f^7$ of the Eu^{2+} ions. Based on the photoluminescence results, the synthesized phosphor may play an important role in making the green-producing phosphor for display devices application. The PL emission in the green region indicated the presence of Eu as Eu^{2+} ions in this sample. The presence of the ions was further confirmed by ESR studies.

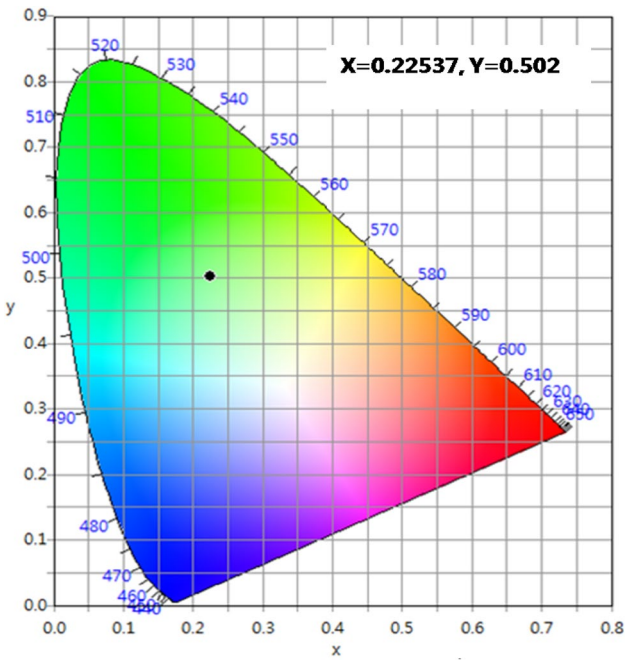

Fig. 7 CIE chromaticity diagram of $SrAl_2O_4$:Eu^{2+} phosphor

Acknowledgements This research was supported by Basic Science Research Program through the National Research Foundation of Korea (NRF) funded by the Ministry of Education (2017R1D1A1B03030003).

References

1. M. Ayvacikli, Z. Kotan, E. Ekdal, Y. Karabulut, A. Canimoglu, J.G. Guinea, A. Khatab, M. Henini, N. Can, Solid state synthesis of $SrAl_2O_4$:Mn^{2+} co-doped with Nd^{3+} phosphor and its optical properties. J. Lumin **144**, 128–132 (2013)
2. I. Mindru, D. Gingasu, L. Patron, G. Marinescu, J.M. Calderon-Moreno, L. Diamandescu, M. Secu, O. Oprea, Tb^{3+}-doped alkaline-earth aluminates: synthesis, characterization and optical properties. Mater. Res. Bull **85**, 240–248 (2017)
3. M.A. Lephoto, O.M. Ntwaeaborwa, S.S. Pitale, H.C. Swart, J.R. Botha, B.M. Mothudi, Synthesis and characterization of $BaAl_2O_4$:Eu^{2+} co-doped with different rare earth ions. Phys. B **407**, 1603–1606 (2012)
4. A.H. Wako, F.B. Dejene, H.C. Swart, Combustion synthesis, characterization and luminescence properties of barium aluminate phosphor. J. Rare Earths **32**, 806–811 (2014)
5. T. Aitasalo, P. Dereń, J. Hölsä, H. Jungner, J.-C. Krupa, M. Lastusaari, J. Legendziewicz, J. Niittykoski, W. Stręk, Persistent luminescence phenomena in materials doped with rare earth ions. J. Solid State Chem **171**, 114–122 (2003)
6. F. Clabau, X. Rocquefelte, S. Jobic, P. Deniard, M.-H. Whangbo, A. Garcia, T. Le Mercier, Mechanism of phosphorescence appropriate for the long-lasting phosphors Eu^{2+}-doped $SrAl_2O_4$ with Codopants Dy^{3+} and B^{3+}, Chem. Mater **17**, 3904–3912 (2005)
7. S.-D. Han, K.C. Singh, T.-Y. Cho, H.-S. Lee, D. Jakhar, J.P. Hulme, C.-H. Han, J.-D. Kim, I-S. Chun, J. Gwak, Preparation and characterization of long persistence strontium aluminate phosphor. J. Lumin **128**, 301–305 (2008)
8. R.E. Rojas-Hernandez, F. Rubio-Marcos, M.V.D. Santos Rezende, M.Á. Rodriguez, A. Serrano, Á. Muñoz-Noval, J.F. Fernandez, The impact of the synthesis conditions on $SrAl_2O_4$:Eu, Dy formation for a persistent afterglow. Mater. Des **108**, 354–363 (2016)
9. J. Li, J. Wang, Y. Yu, Y. Zhu, M. Ge, Preparation and luminescence properties of rare-earth doped fiber with spectral blue-shift: $SrAl_2O_4$:Eu^{2+},Dy^{3+} phosphors/triarylsulfonium hexafluoroantimonate based on polypropylene substrate. J. Rare Earths **35**, 530–535 (2017)
10. Y. Murayama, N. Takeuchi, Y. Aoki, T. Matsuzawa, U.S. Patent No. 5,424,006, 1995
11. E. Shafia, A. Aghaei, M. Bodaghi, M. Tahriri, Combusion synthesis, structural and photo-physical characteristics of Eu^{2+} and Dy^{3+} co-doped $SrAl_2O_4$ phosphor nanopowders. J. Mater. Sci. **22**, 1136–1142 (2011)
12. X.Y. Chen, C. Ma, X. Xiao, C.W. Li, X.L. Shi, D.R. Li, Lu, Novel necklace-like MAl_2O_4:Eu^{2+}, Dy^{3+} (M = Sr, Ba, Ca) phosphors via a CTAB-assisted solution-phase synthesis and postannealing approach. J. Phys. Chem. C **113**, 2685–2689 (2009)

13. Q. Xiao, L. Xiao, Y. Liu, X. Chen, Y. Li, Synthesis and luminescence properties of needle-like $SrAl_2O_4$:Eu, Dy phosphor via a hydrothermal co-precipitation method. J. Phys. Chem. Solids **71**, 1026–1030 (2010)
14. Z. Győri, V. Havasi, D. Madarász, D. Tátrai, T. Brigancz, G. Szabó, Z. Kónya, Á. Kukovecz, Luminescence properties of Ho^{3+} co-doped $SrAl_2O_4$:Eu^{2+}, Dy^{3+} long-persistent phosphors synthesized with a solid-state method. J. Mol. Struct **1044**, 87–93 (2013)
15. Z. Xue, S. Deng, Y. Liu, B. Lei, Y. Xiao, M. Zheng, Synthesis and luminescence properties of $SrAl_2O_4$:Eu^{2+},Dy^{3+} hollow microspheres via a solvothermal co-precipitation method. J. Rare Earths **31**, 241–246 (2013)
16. E. Shafia, M. Bodaghi, S. Esposito, A. Aghaei, A critical role of pH in the combustion synthesis of nano-sized $SrAl_2O_4$:Eu^{2+}, Dy^{3+} phosphor. Ceram. Int **40**, 4697–4706 (2014)
17. Y. Liu, C.-N. Xu, Influence of calcining temperature on photoluminescence and triboluminescence of europium-doped strontium aluminate particles prepared by a sol-gel process. J. Phys. Chem. B **107**, 3991–3995 (2003)
18. W. Chung, H.J. Yu, S.H. Park, B.-H. Chun, J. Kim, S.H. Kim, Spray pyrolysis synthesis of MAl_2O_4:Eu^{2+} (M = Ba, Sr) phosphor for UV LED excitation. J. Cryst. Growth **326**, 73–76 (2011)
19. C.-H. Lu, S.-Y. Chen, C.H. Hsu, Nanosized strontium aluminate phosphors prepared via a reverse microemulsion route. Mater. Sci. Eng. B **140**, 218–221 (2007)
20. J Zhong, D Chen, Y Yuan, L Chen, Z Ji, Synthesis and spectroscopic investigation of $Ba_3La_6(SiO_4)_6$:Eu^{2+} green phosphors for white light-emitting diodes. Chem. Eng **309**, 795–801 (2017)
21. Y. Xia, Y.-G. Liu, Z. Huang, M. Fang, M.S. Molokeevbc, L.F. Mei, $Ca_6La_4(SiO_4)_2(PO_4)_4O_2$:$Eu^{2+}$:a novel apatite green-emitting phosphor for near-ultraviolet excited w-LEDs. J. Mater. Chem. C **4**, 4675–4683 (2016)
22. W. Lü, Z. Hao, X. Zhang, Y. Liua, Y. Luo, X. Liu, X. Wang, J.Zhang, Eu^{2+}-Activated $Ca_8Zn(SiO_4)_4Cl_2$: an intense green emitting phosphor for blue light emitting diodes. J. Electrochem. Soc **158**, H124–H127 (2011)
23. T. Komukai, Y. Sato, H. Kato, M. Kakihana, A high-luminescence $BaZrSi_3O_9$:Eu^{2+} blue–green-emitting phosphor: Synthesis and mechanism. J. Lumin. **181**, 211–216 (2017)
24. C. Li, H. Chen, S. Xu, Ba3 $Si_6O_{12}N_2$:Eu^{2+} green-emitting phosphor for white light emitting diodes: luminescent properties optimization and crystal structure analysis. Optik **126**, 499–502 (2015)
25. R.E. Rojas-Hernandez, F. Rubio-Marcos, R. Henrique Goncalves, M. Ángel Rodriguez, E. Veron, M.´, C. Allix, J.F. Bessada, Fernandez, Original synthetic route to obtain a $SrAl_2O_4$ phosphor by the molten salt method: insights into the reaction mechanism and enhancement of the persistent luminescence. Inorg. Chem. **54**, 9896–9907 (2015)
26. K.-S. Hwang, B.-A. .Kang, S.-D. Kim, S. Hwangbo, J.-T. Kim, Cost-effective electrostatic-sprayed $SrAl_2O_4$:Eu^{2+} phosphor coatings by using salted sol–gel derived solution. Bull. Mater. Sci. **34**, 1059–1062 (2011)
27. M. Misevicius, O. Scit, I. Grigoraviciute-Puroniene, G. Degutis, I. Bogdanoviciene, A. Kareiva, Sol-gel synthesis and investigation of un-doped and Ce-doped strontium aluminates. Ceram. Int. **38**, 5915–5924 (2012)
28. L.E. Iton, J. Turkevich, Electron paramagnetic resonance of rare earth ions in zeolites. J. Phys. Chem **81**, 435–449 (1977)
29. L.E. Iton, C.M. Brodbeck, S.L. Suib, G.D. Stucky, EPR study of europium ions in type A zeolite. The general classification of the EPR spectra of Sstate rare-earth ions in disordered polycrystalline or glassy matrices. J. Chem. Phys. **79**, 1185–1196 (1983)
30. C.M. Brodbeck, L.E. Iton, The EPR spectra of Gd^{3+} and Eu^{2+} in glassy systems. J. Chem. Phys. **83**, 4285–4299 (1985)
31. A. Schulze, H. Mueller-Buschbaum, Zur Verbindungsbildung von MeO: M_2O_3. IV. Zur Struktur von monoklinem $SrAl_2O_4$, Z. Anorg. Allg. Chem. **475**, 205–210 (1981)
32. M.M. Kuklja, Defects in yttrium aluminium perovskite and garnet crystals: atomistic study. J. Phys. **12**, 2953–2967 (2000)
33. A.P. Patel, M.R. Levy, R.W. Grimes, R.M. Gaume, R.S. Frigelson, K.J. McClellan, C.R. Stanek, Mechanisms of nonstoichiometry in $Y_3Al_5O_{12}$. Appl. Phys. Lett. **93**, 191902 (2008)
34. J. Dong, K. Lu, Noncubic symmetry in garnet structures studied using extended X-ray-absorption fine-structure spectra. Phys. Rev. B **43**, 8808–8821 (1991)
35. D. Truong, M.K. Devaraju, T. Tomai, I. Honma, Direct observation of antisite defects in $LiCoPO_4$ cathode materials by annular dark- and bright-field electron microscopy. ACS Appl. Mater. Interfaces **5**, 9926–9932 (2013)
36. T. Aitasalo, J. Hölsä, H. Jungner, J.-C. Krupa, M. Lastusaari, J. Legendziewicz, J. Niittykoski, Effect of temperature on the luminescence processes of $SrAl_2O_4$:Eu^{2+}. Radiat. Meas **38**, 727–730 (2004)
37. R.D. Shannon, Revised effective ionic radii and systematic studies of interatomic distances in halides and chalcogenides. Acta Cryst. A. **32**, 751–767 (1976)
38. N. Yuan, X. Liu, F. Meng, D. Zhou, J. Meng, First-principles study of La_2CoMnO_6: a promising cathode material for intermediate-temperature solid oxide fuel cells due to intrinsic Co-Mn cation disorder. Ionics. 21, 1675–1681 (2015)
39. R. Ravichandran, S.T. Johnson, S. Erdei, R. Roy, W.B. White, Crystal chemistry and luminescence of the Eu^{2+}-activated alkaline earth aluminate phosphors. Displays. 19 (1999) 197–203
40. Y.K. Song, S.K. Choi, H.S. Moon, T.W. Kim, S.I. Mho, H.L. Park, Phase studies of SrO-Al_2O_3 by emission signatures of Eu^{2+} and Eu^{3+}. Mater. Res. Bull. **32**, 337–341 (1997)
41. F.C. Palilla, A.K. Levine, M.R. Tomkus, Fluorescent properties of alkaline earth aluminates of the type MAl_2O_4 activated by divalent europium. J. Electrochem. Soc. **115**, 642–644 (1968)